

*The clinopyroxenes of the Skaergaard intrusion,  
eastern Greenland.*

By I. D. MUIR, B.A., Ph.D., F.G.S.

Department of Mineralogy and Petrology, University of Cambridge.

[Read March 23, 1950.]

---

I. INTRODUCTION.

**D**URING the past twenty years considerable attention has been given to the compositions of the pyroxenes from basic igneous rocks. Hess (1941) reviewed the courses of crystallization of pyroxenes from mafic magmas and drew a trend line for the lime-rich clinopyroxenes. The present investigation was undertaken primarily to determine more closely the trend in the ferroaugite region, for here Hess's trend was based on the analyses of two pyroxenes from the Skaergaard intrusion and both of these are now known to be somewhat unusual types. The Skaergaard intrusion which is a strongly fractionated gabbroic complex is particularly suitable for this study of the ferroaugites. Fifteen new analyses have been made for this investigation and twenty-three analyses of the pyroxenes from this intrusion are now available. Using nineteen of these, new trend lines have been drawn (fig. 1) for the Skaergaard clinopyroxenes.

The Skaergaard intrusion of east Greenland, Tertiary in age, was described by Wager and Deer in 1939. They showed it to be a strongly differentiated layered gabbro complex having the form of an inverted cone. A uniform chilled margin to the border group gives the composition of the original magma. This rock is an olivine-gabbro of tholeiitic type (Tilley, 1951) chemically similar to the porphyritic central magma type of the British Tertiary Hebridean province. The rocks of the layered series range from hypersthene-olivine-gabbros in the lowest exposed rocks to fayalite-quartz-gabbros at the top.

Wager and Deer (1938, 1939) have published analyses of eight clinopyroxenes from this intrusion, five of which came from the layered series. They investigated the mutual relations of the clino- and orthopyroxenes in the rocks, concluding that in the earlier rocks both ortho- and clinopyroxene crystallized, but that in the middle gabbros it may have been

that clinopyroxene alone crystallized from the magma and that some inverted to orthopyroxene with abundant clinopyroxene inclusions. In the latest stages pyroxenes with very unusual textures for igneous pyroxenes occur and the authors suggested that these were really inverted forms, having crystallized from the magma as iron-wollastonites. The new chemical data have confirmed the suggestions of Wager and Deer regarding the inversion origin of these pyroxenes.

In their discussion on the trend of the pyroxenes Wager and Deer considered that in the early stages two pyroxenes (diopsidic augite and orthopyroxene), crystallized out, and, with progressive fractionation of the magma, both became enriched in iron, while at the same time the clinopyroxene became progressively poorer in lime. Eventually orthopyroxene ceased to crystallize and they considered that this was due to the increasing capacity of the clinopyroxene to take the whole of the pyroxene components into solid solution as the iron content increased. Thus, towards the iron-rich end, the immiscibility gap between lime-rich clinopyroxenes and pigeonites narrowed and eventually, beyond Of (orthoferrosilite) 65–70, only one moderately lime-poor phase crystallized. They termed such pyroxenes 'clinopyroxenes of pigeonite type'.

Hess (1941) pointed out that these iron-rich clinopyroxenes of the Skaergaard intrusion were not true pigeonites, but rather, iron-rich members of the augite series, i.e. ferroaugites. He considered that the field of orthopyroxene (in this case inverted pigeonite) was limited by the incoming and enlargement of the olivine field as the magmatic liquid became increasingly rich in iron.

The additional analyses carried out for this paper have revealed that the trend of the clinopyroxenes shows two abrupt changes in direction. These coincide with the disappearance of olivine as an orthomagmatic mineral at the top of the hypersthene-olivine-gabbros (height 900 metres in the layered series) and with its later reappearance in the lower ferro-gabbros (height 1400 metres in the layered series).

The early clinopyroxenes found in the hypersthene-olivine-gabbros are lime-rich diopsidic augites. In the olivine-free middle gabbros, which succeed the hypersthene-olivine-gabbros, the composition of the clinopyroxene becomes increasingly poorer in lime and richer in iron. In the lower ferrogabbros the lime content of the clinopyroxene increases again. With increasing iron content the trend of compositions of the normal ferroaugites turns towards hedenbergite with their lime content maintaining a gradual increase. The clinopyroxenes formed by the iron-wollastonite-hedenbergite inversion, however, become increasingly more

iron-rich and lime-poor over the range in which they crystallize and thus in the latest stages two distinct trends can be recognized.

In this paper the author has followed Hess (1949) in expressing the compositions of the clinopyroxenes as atomic percentages in terms of the Ca, Mg, and total Fe components. A complete description of the rocks and their textures is given by Wager and Deer (1939).

## II. DISCUSSION OF ANALYSES.

In the earlier rocks of the intrusion, where two pyroxenes occur, it was not possible to effect a separation of the two minerals and the mixed pyroxenes of the rock were therefore analysed (table I). Analyses 18

TABLE I. Analyses of mixed pyroxenes.

Analysis no.	2.	5.	6.	7.	8.	9.	A.	B.
SiO <sub>2</sub> ...	50.58	51.66	49.89	47.66	48.97	47.92	46.29	46.05
Al <sub>2</sub> O <sub>3</sub> ...	4.06	2.44	3.74	3.48	3.85	4.60	2.26	1.17
TiO <sub>2</sub> ...	0.55	0.99	0.93	0.81	0.81	1.71	0.74	0.66
Fe <sub>2</sub> O <sub>3</sub> ...	1.39	0.60	0.21	0.38	2.18	0.71	1.36	0.60
FeO ...	11.07	9.37	12.81	14.57	11.93	18.85	29.68	31.10
MnO ...	0.25	0.15	0.27	0.30	0.28	0.35	0.90	0.78
MgO ...	22.07	15.14	14.59	13.45	13.96	12.03	0.69	1.01
CaO ...	10.01	18.74	16.83	17.94	17.36	12.95	16.07	17.64
Na <sub>2</sub> O ...	0.16	0.46	0.43	0.42	0.38	0.51	0.73	0.73
K <sub>2</sub> O ...	0.01	0.14	0.13	0.18	0.21	0.13	0.19	0.19
H <sub>2</sub> O+ ...	0.16	0.11	0.16	0.11	0.12	0.20	0.43	0.43
H <sub>2</sub> O- ...	0.09	0.11	0.07	0.11	0.11	0.18	0.20	0.20
	100.40	99.91	100.06	99.41	100.16	100.14	99.54	100.56

A. Fraction consisting of 96 % green pyroxene from rock 4143.

B. Fraction consisting of 48 % brown pyroxene from rock 4143.

See foot of table II.

and 22 (table II) represent the brown and the green pyroxenes respectively occurring together in a rock at a height of 2400 metres in the layered series. The refractive indices of the two varieties are similar, but the optic axial angle is 55° for the brown variety and 52° for the green. An attempt was made to separate the two varieties and by repeated centrifuging two fractions were obtained, the heavier (analysis A, table I) consisting of 96 % of the green, and the lighter (analysis B, table I) about 48 % of the brown.

In general, there is a decrease in the silica weight percentage of the pyroxenes as the layered series is ascended, and this is due to the replacement of Mg by Fe". Aluminium, at its maximum in the pyroxene of the chilled margin, remains fairly constant in the earlier augites, but

TABLE II. Analyses and optical properties of clinopyroxenes.

	1.	2a.	5b.	6c.	7d.	8e.
SiO <sub>2</sub> ... ..	49.84	49.98	51.48	48.98	46.80	48.60
Al <sub>2</sub> O <sub>3</sub> ... ..	6.22	4.49	2.87	4.67	4.56	4.26
TiO <sub>2</sub> ... ..	0.90	0.61	1.16	1.16	1.07	0.90
Fe <sub>2</sub> O <sub>3</sub> ... ..	2.86	1.53	0.70	0.25	0.50	2.41
FeO ... ..	8.67	9.81	6.26	9.89	9.89	9.85
MnO ... ..	0.23	0.28	0.18	0.33	0.39	0.31
MgO ... ..	12.67	21.76	14.35	12.72	12.29	13.57
CaO ... ..	17.80	11.07	22.04	21.02	23.43	19.20
Na <sub>2</sub> O ... ..	0.38	0.18	0.54	0.53	0.56	0.42
K <sub>2</sub> O ... ..	0.05	0.01	0.16	0.16	0.23	0.23
H <sub>2</sub> O+ ... ..	0.18	0.18	0.13	0.20	0.14	0.13
H <sub>2</sub> O- ... ..	0.07	0.10	0.13	0.09	0.14	0.12
	99.87	100.00	100.00	100.00	100.00	100.00
$\alpha$ ... ..	1.695	1.672	1.690	1.695	1.700	1.698
$\beta$ ... ..	—	1.678	1.696	1.702	1.706	1.705
$\gamma$ ... ..	1.719	1.701	1.718	1.722	1.730	1.724
$\gamma-\alpha$ ... ..	0.024	0.029	0.028	0.027	0.030	0.026
2V $\gamma$ ... ..	43°	42°	42°	43°	42°	40°
$\gamma:c$ ... ..	41°	39°	40°	41°	36°	40°
Sp. gr. ... ..	—	3.35	3.34	3.38	3.38	3.38
Atomic %						
Ca ... ..	40	22	46	45	49	40
Mg ... ..	38	60	42	37.5	33	40
Fe ... ..	22	18	12	17.5	18	20
$\frac{\text{FeO} + \text{Fe}_2\text{O}_3 \times 100}{\text{MgO} + \text{FeO} + \text{Fe}_2\text{O}_3}$						
mineral ... ..	46	34	33	43	46	47
rock ... ..	55	49	—	55	—	—
	9f.	10.	11.	12A.	13.	14.
SiO <sub>2</sub> ... ..	47.55	48.79	49.38	49.38	49.03	47.70
Al <sub>2</sub> O <sub>3</sub> ... ..	5.01	1.91	0.93	2.93	0.75	1.55
TiO <sub>2</sub> ... ..	1.86	1.00	0.79	0.71	0.85	1.24
Fe <sub>2</sub> O <sub>3</sub> ... ..	0.78	2.90	2.09	1.48	3.07	1.82
FeO ... ..	17.56	18.13	18.46	17.36	18.62	20.32
MnO ... ..	0.38	0.17	0.29	0.23	0.31	0.38
MgO ... ..	11.63	11.06	10.98	10.66	10.16	8.73
CaO ... ..	14.12	15.58	16.43	16.83	16.79	17.32
Na <sub>2</sub> O ... ..	0.55	0.43	0.59	0.37	0.47	0.65
K <sub>2</sub> O ... ..	0.14	0.26	0.07	0.11	0.13	0.13
H <sub>2</sub> O+ ... ..	0.22	0.12	0.19	0.15	0.17	0.21
H <sub>2</sub> O- ... ..	0.20	0.14	0.15	0.07	0.14	0.11
	100.00	100.49	100.35	100.28	100.49	100.16
$\alpha$ ... ..	1.707	1.704	1.704	1.709	1.712	1.718
$\beta$ ... ..	1.715	1.712	1.711	1.713	—	1.725
$\gamma$ ... ..	1.735	1.733	1.733	1.739	1.738	1.741

TABLE II (cont.)

$\gamma-\alpha$	...	...	0.028	0.029	0.029	0.030	0.026	0.023
$2V_\gamma$	...	...	40°	45°	45°	46°	52°	52°
$\gamma:c$	...	...	40°	39°	41°	44°	43°	43°
Sp. gr.	...	...	3.42	—	—	3.49	3.50	3.51
Atomic %								
Ca	...	...	31	33	34	36	35	37
Mg	...	...	36	33	32	32	29	26
Fe	...	...	33	34	34	32	35	37
$\text{FeO} + \text{Fe}_2\text{O}_3 \times 100$								
$\text{MgO} + \text{FeO} + \text{Fe}_2\text{O}_3$								
mineral	...	...	61	66	65	64	68	72
rock	...	...	70	—	—	79	—	86
<hr/>								
			15.	16.	17.	18.	19.	20.
$\text{SiO}_2$	...	...	47.45	46.06	47.20	45.05	46.54	—
$\text{Al}_2\text{O}_3$	...	...	2.57	4.06	1.90	nil	5.77	—
$\text{TiO}_2$	...	...	1.14	1.58	1.21	0.55	1.22	—
$\text{Fe}_2\text{O}_3$	...	...	2.83	1.21	1.26	nil	1.88	—
FeO	...	...	21.54	24.02	27.43	31.76	24.65	—
MnO	...	...	0.45	0.42	0.20	0.64	0.74	—
MgO	...	...	6.30	4.51	2.54	1.35	0.79	—
CaO	...	...	16.83	17.37	17.78	19.09	17.70	—
$\text{Na}_2\text{O}$	...	...	0.64	0.53	0.56	0.73	0.62	—
$\text{K}_2\text{O}$	...	...	0.25	0.21	0.26	0.20	0.15	—
$\text{H}_2\text{O}^+$	...	...	0.30	0.21	0.29	0.43	0.39	—
$\text{H}_2\text{O}^-$	...	...	0.18	0.12	0.11	0.20	0.18	—
			100.48	100.30	100.74	100.00	100.63	—
$\alpha$	...	...	1.719	1.735	1.737	1.745	1.726	1.728
$\beta$	...	...	1.726	1.741	1.741	—	1.732	1.735
$\gamma$	...	...	1.747	1.761	1.765	1.770	1.753	1.756
$\gamma-\alpha$	...	...	0.028	0.026	0.028	0.025	0.027	0.028
$2V_\gamma$	...	...	47°	51°	50°	55°	49°	56°
$\gamma:c$	...	...	47°	40°	43°	—	44°	—
Sp. gr.	...	...	—	—	—	—	3.48	—
Atomic %								
Ca	...	...	38	38	41	41	44	—
Mg	...	...	20	14	8	4	3	—
Fe	...	...	43	48	51	55	53	—
$\text{FeO} + \text{Fe}_2\text{O}_3 \times 100$								
$\text{MgO} + \text{FeO} + \text{Fe}_2\text{O}_3$								
mineral	...	...	79	84	92	96	97	—
rock	...	...	—	94	—	—	98	—
<hr/>								
			21.	22.	23.	3.	4.	12.
$\text{SiO}_2$	...	...	45.93	46.60	42.62	50.39	49.68	42.32
$\text{Al}_2\text{O}_3$	...	...	2.25	2.37	5.24	3.54	4.99	2.25
$\text{TiO}_2$	...	...	0.71	0.75	1.69	0.87	1.17	4.42
$\text{Fe}_2\text{O}_3$	...	...	1.98	1.42	3.74	1.95	1.12	4.72

TABLE II (cont.)

FeO	...	...	28.94	29.70	31.54	8.47	11.76	25.13
MnO	...	...	1.16	0.92	0.78	0.19	0.16	0.22
MgO	...	...	0.79	0.67	0.47	15.82	12.79	8.33
CaO	...	...	15.54	16.01	12.27	18.41	17.97	12.07
Na <sub>2</sub> O	...	...	0.78	0.73	1.02	0.70	0.56	0.61
K <sub>2</sub> O	...	...	0.21	0.20	0.23	0.14	0.13	trace
H <sub>2</sub> O+	...	...	0.44	0.43	0.48	0.11	0.18	0.12
H <sub>2</sub> O-	...	...	0.22	0.20	0.22	0.04	0.15	0.25
			98.95	100.00	100.30	100.63	100.66	100.44
$\alpha$	...	...	1.747	1.745	1.743	1.684	1.690	1.721
$\beta$	...	...	1.754	1.753	1.751	1.692	1.697	1.728
$\gamma$	...	...	1.772	1.771	1.772	1.712	1.716	1.749
$\gamma-\alpha$	...	...	0.025	0.026	0.029	0.028	0.026	0.028
$2V_{\gamma}$	...	...	50°	52°	58°	46°	42-52°	44°
$\gamma:c$	...	...	39°	41°	47°	39°	38°	39°
Sp. gr.	...	...	—	—	3.65	3.35	3.37	3.50
Atomic %								
Ca	...	...	37.5	38	30	38	39	26
Mg	...	...	2.5	2	2	45	39	32
Fe	...	...	60	59	68	17	22	49
$\text{FeO} + \text{Fe}_2\text{O}_3 \times 100$								
$\text{MgO} + \text{FeO} + \text{Fe}_2\text{O}_3$								
mineral	...	...	98	98	99	40	49	87
rock	...	...	99	—	96	—	—	79

## KEY TO TABLES I AND II

- Pyroxene from chilled margin. Rock no. 1724.
- Augite from transitional layered series. Rock 4087.
- „ „ lower border group. Rock 4289.
- Pyroxene from border group. Rock 1222.
- „ „ hypersthene-olivine-gabbro, height 300 metres (Rock 4084).
- „ „ „ „ „ „ 500 m. (4077).
- „ „ „ „ „ „ 700 m. (2307).
- „ „ „ middle gabbro, height 1100 m. (1691).
- „ „ „ „ „ „ 1150 (3662).
- Ferroaugite from hortonolite-ferrogabbro, height 1600 m. (2580).
- „ „ „ „ „ „ 1700 m. (2573).
- „ „ „ „ „ „ 1800 m. (1907).
- 12s. „ „ „ „ „ „ 1800 m. (1907).
- „ „ „ „ „ „ 1900 m. (4265).
- „ „ „ „ „ „ 2000 m. (4272).
- „ „ „ ferrohortonolite-ferrogabbro, height 2100 m. (4146).
- „ „ „ „ „ „ 2200 m. (4145).
- „ „ „ „ „ „ 2300 m. (4144).
- Brown pyroxene from ferrohortonolite-ferrogabbro, height, 2400 m. (4143).
- Green pyroxene from unlaminate layered series, height 2750 m. (4136).
- „ „ „ „ transgressive granophyre (1223).
- „ „ „ „ ferrohortonolite-ferrogabbro, height 2375 m. (1974).
- „ „ „ „ „ „ 2400 m. (4143).
- „ „ „ „ fayalite-ferrogabbro „ 2500 m. (1881).

TABLE II (*cont.*)

Note.—All refractive indices  $\pm 0.002$ .  $2V$  and  $\gamma:c \pm 2^\circ$ .

Pyroxene numbers	1-8	colour light brown; pleochroism weak.
" "	9-18	colour brownish; pleochroism weak. $\alpha$ yellow-brown, $\beta$ violet-brown, $\gamma$ violet-brown.
" "	19-20	pale greenish-brown, pleochroism weak,
" "	21-23	greenish; pleochroism, $\alpha$ pale green, $\beta$ green, $\gamma$ green.
a,	(Clinopyroxene, analysis 2,	after subtracting 9.6 % hypersthene (Of 41) and recalculating to 100 %.
b,	" "	5, after subtracting 14.8 % hypersthene (Of 44) and recalculating to 100%.
c,	" "	6, after subtracting 20 % hypersthene (Of 45) and recalculating to 100 %.
d,	" "	7, after subtracting 23 % hypersthene (Of 49) and recalculating to 100%.
e,	" "	8, after subtracting 9.8 % hypersthene (Of 50) and recalculating to 100 %.
f,	" "	9, after subtracting 9.4 % hypersthene (Of 58) and recalculating to 100%.

Analyses 2, 3, 4, 6, 9, 12, 19, and 23 by W. A. Deer (Wager and Deer, 1939).

Analyses 1, 5, 7, 8, 10, 11, 12A, 13, 14, 15, 16, 17, 18, 21, and 22 by I. D. Muir.

later shows a general tendency to decrease. It might be considered that the higher alumina in the recalculated analyses could be attributed to its presence in the associated orthopyroxene, for no allowance was made for this constituent in the subtraction. In the Skaergaard rocks selected, however, orthopyroxene never exceeds one quarter of the total pyroxene, and a survey of recent reliable analyses indicated that orthopyroxenes seldom carry much in excess of 2 %  $Al_2O_3$ . It is clear, therefore, that the bulk of the alumina of the analysis must be present in the monoclinic variety. Titania shows a general tendency to increase from about 1 % in the earlier pyroxenes to 1.5 % in the later ones, but the behaviour of this constituent can be demonstrated much more clearly when considered in relation to the structure. Both manganese and total alkalis also show a general tendency to increase in the later pyroxenes, as does ferric iron.

An attempt was made to separate the pyroxene from a contaminated rock of the border group where hypersthene-olivine-gabbro is hybridized by the country gneiss. These hybrids become very coarse-grained, having pyroxene crystals up to 10 mm. in length. These, and strongly zoned plagioclase crystals, are set in a granophyric groundmass. From the evidence of drusy cavities, volatile constituents were clearly present in many of the granophyre hybrids and it seems likely that a vapour phase separated at a late stage in the crystallization.

G. C. Kennedy (1949), discussing equilibrium relations between iron oxides and volatiles in igneous rocks, has shown experimentally that the

$\text{Fe}_2\text{O}_3:\text{FeO}$  ratio in a rock melt depends on the partial pressure of oxygen with which the melt is in equilibrium and that the reaction  $2\text{Fe}_2\text{O}_3 \rightleftharpoons 4\text{FeO} + \text{O}_2$  may be expressed as a close approximation by the law of mass action. From this it follows that at any given temperature an increase in the partial pressure of oxygen should drive the reaction to the left. With falling temperature, however, and a constant partial pressure of oxygen, the reaction would tend to proceed to the right. In other words, at a lower temperature a greater increase in the partial pressure of oxygen is required to increase the  $\text{Fe}_2\text{O}_3:\text{FeO}$  ratio. No analysis of the granophyre is available, but considerable magnetite is present in the rock. It was thought that the composition of the pyroxene might give an indication of whether this increase in the  $\text{Fe}_2\text{O}_3:\text{FeO}$  ratio took place in the magma. The optical properties of the pyroxene are  $\alpha$  1.692,  $\gamma$  1.722,  $2V$   $52^\circ$  (centre) and  $49^\circ$  (margins). As much of the pyroxene has been converted to a pale amphibole, it was impossible to separate sufficient pure material for an accurate analysis, but on 0.35 gram separated and with about 5 % of green amphibole remaining, the figures obtained were FeO 10.41,  $\text{Fe}_2\text{O}_3$  7.77 %. These tend to support the views put forward by Kennedy. Another feature of the analysis of the pyroxene worthy of mention is that hybridization of hypersthene-olivine-gabbro with the gneiss produces a pyroxene in hybrid rocks whose composition, except for the  $\text{Fe}_2\text{O}_3:\text{FeO}$  ratio, is similar to those from the middle gabbros.

The most marked feature of the analyses is the complementary variation in magnesium and ferrous iron. When plotted against height in the layered series both MgO and FeO form smooth curves. The replacement of magnesium by ferrous iron in progressively later pyroxenes is now well known. The other important variable in the analyses is the lime content. In the layered series the lime content of the augites remains almost constant during the hypersthene-olivine-gabbro stage, but in the middle gabbros the clinopyroxenes become increasingly lime-poor and lie in the field of augites from olivine-free tholeiitic rocks. In the early ferrogabbros, however, the lime content increases again, and the only comparison with this known to the author is that shown by the later pyroxenes of the New Amalfi sheet described by Poldervaart (1944), where pyroxenes remarkably similar in texture to the inverted varieties occur. It will be noted that the lime content decreases again in the green pyroxenes considered to have formed by inversion from iron-wollastonite, whereas in the normal brown pyroxenes it increases until in the latest stages the composition approaches closely to hedenbergite.

### III. THE CRYSTAL CHEMISTRY OF THE PYROXENES.

Warren and Bragg (1928) first worked out the structure of diopside, and Warren and Bischof (1931) showed that diopside, hedenbergite, acmite, jadeite, spodumene, augite, and clinoenstatite had essentially similar structures of which diopside could be taken as the type. They suggested as a general formula for members of the pyroxene group  $X_m Y_{(2-m)} z_2(O, OH, F)_6$ ; where  $X = Ca, Na, (K), (Mn), (Mg), Y = Mg, Fe'', Mn, Fe''', Ti, Al, (Zn), z = Si, Al$ .

Dixon and Kennedy (1933) showed that in some cases it was necessary to assume a replacement of silicon by titanium in order to make the analysis fit the formula. They listed a number of analyses in which combined silicon and aluminium was insufficient to supply the  $z$  group in the centre of the tetrahedron. Barth (1931) came to a similar conclusion with regard to the titaniferous pyroxene from Hiva Oa, as did Deer and Wager (1938) for pyroxene no. 12 of the Skaergaard intrusion.

The early clinopyroxenes are normal gabbroic types with more than sufficient aluminium to satisfy the silicon deficiency in the tetrahedral positions, and some must therefore be present in the  $Y$  group. This condition appears to hold to the end of the middle gabbro stage, but in the pyroxenes of the early ferrogabbros there is insufficient aluminium to satisfy the requirements of the  $z$  group, and in pyroxene no. 10 titanium is required to bring this group up to 2 (table III). A similar assumption must be made to balance the electrostatic charges for pyroxenes 11, 12, 13, and 14. In pyroxene no. 15 there is just sufficient aluminium present to satisfy the  $z$  group, and in no. 16 and all succeeding analyses aluminium is again in excess and some must be present in the  $Y$  group. It would appear, therefore, that over a limited range of the ferrogabbros titanium occupies positions in the  $z$  group of the pyroxenes.

In the analyses where no aluminium occurs in the  $Y$  group there is an increase in the content of ferric iron in the pyroxenes, and this replacement of  $Fe''$  by  $Fe'''$  is required to balance the substitution of Al for Si. Thus in analyses 10, 11, 12, 13, and 14, ferric iron is present in much greater amount than in the other pyroxenes, except for the inverted ones where a high ferric iron content is required partly to balance the aluminium and partly to offset the substitution of sodium and potassium for calcium in the  $X$  group, for the alkalis show a significant increase at this stage.

In the three earliest analyses from the layered series the  $(Ca + Na + K)$  comprising the  $X$  group remains fairly constant at about 0.9. At this stage, therefore, any replacements that occur must be due to the

TABLE III. Formulac of pyroxenes on basis of six oxygen atoms.

		1.	2.	5.	6.	7.	8.	9.	10.
z	Si ...	1.857	1.836	1.911	1.822	1.793	1.840	1.833	1.889
	Al ...	0.143	0.165	0.089	0.178	0.207	0.160	0.167	0.086
	Ti ...	—	—	—	—	—	—	—	0.025
Y	Al ...	0.133	0.029	0.032	0.027	—	0.031	0.060	—
	Ti ...	0.025	0.017	0.033	0.032	0.032	0.025	0.054	0.006
	Fe <sup>m</sup> ...	0.082	0.043	0.018	0.007	0.021	0.068	0.023	0.084
	Fe <sup>s</sup> ...	0.269	0.301	0.198	0.308	0.315	0.311	0.566	0.558
	Mn ...	0.006	0.009	0.007	0.010	0.013	0.008	0.012	0.004
	Mg ...	0.675	0.190	0.759	0.705	0.706	0.776	0.668	0.645
X	Ca ...	0.717	0.435	0.877	0.837	0.961	0.777	0.583	0.649
	Na ...	0.023	0.013	0.044	0.038	0.041	0.027	0.033	0.036
	K ...	0.002	—	0.013	0.007	0.009	0.009	0.007	0.014
z ...	2.00	2.00	2.00	2.00	2.00	2.00	2.00	2.00	
XY ...	1.94	2.04	1.98	1.97	2.10	2.03	2.01	2.00	
		11.	12a.	13.	14.	15.	16.	17.	18.
z	Si ...	1.916	1.905	1.920	1.886	1.881	1.850	1.918	1.916
	Al ...	0.042	0.095	0.037	0.074	0.119	0.150	0.082	—
	Ti ...	0.031	—	0.026	0.037	—	—	—	0.022
Y	Al ...	—	0.011	—	—	—	0.042	0.011	—
	Ti ...	—	0.021	—	—	0.033	0.047	0.036	—
	Fe <sup>m</sup> ...	0.062	0.042	0.089	0.049	0.086	0.036	0.039	—
	Fe <sup>s</sup> ...	0.595	0.560	0.573	0.672	0.712	0.804	0.926	1.122
	Mn ...	0.009	0.007	0.010	0.012	0.014	0.014	0.007	0.022
	Mg ...	0.639	0.618	0.604	0.520	0.376	0.271	0.155	0.089
X	Ca ...	0.685	0.694	0.703	0.736	0.717	0.747	0.773	0.847
	Na ...	0.046	0.029	0.037	0.050	0.043	0.041	0.049	0.056
	K ...	0.004	0.004	0.004	0.007	0.014	0.011	0.015	0.010
z ...	1.99	2.00	1.98	2.00	2.00	2.00	2.00	1.94	
XY ...	2.04	1.99	2.02	2.05	2.00	2.01	2.01	2.14	
		19.	21.	22.	23.	3.	4.	12.	
z	Si ...	1.867	1.928	1.925	1.785	1.836	1.862	1.720	
	Al ...	0.133	0.072	0.075	0.215	0.152	0.138	0.107	
	Ti ...	—	—	—	—	—	—	0.135	
Y	Al ...	0.145	0.039	0.045	0.043	—	0.083	—	
	Ti ...	0.037	0.022	0.025	0.053	0.024	0.033	—	
	Fe <sup>m</sup> ...	0.057	0.062	0.045	0.118	0.053	0.039	0.144	
	Fe <sup>s</sup> ...	0.827	1.012	1.030	1.105	0.258	0.369	0.853	
	Mn ...	0.025	0.041	0.035	0.028	0.006	0.005	0.008	
	Mg ...	0.048	0.050	0.042	0.029	0.859	0.714	0.503	
X	Ca ...	0.761	0.698	0.709	0.550	0.719	0.721	0.525	
	Na ...	0.048	0.063	0.055	0.083	0.049	0.041	0.048	
	K ...	0.008	0.011	0.010	0.012	0.008	0.006	—	
z ...	2.00	2.00	2.00	2.00	1.99	2.00	1.96		
XY ...	1.96	2.00	1.99	2.02	1.99	2.01	2.08		

substitution of Mg by Fe<sup>''</sup>. In the middle gabbros, however, the *X* group decreases sharply to 0.62 in pyroxene no. 9, and here the iron introduced must be replacing the calcium, for magnesium remains almost constant. In the lower ferrogabbros (analyses 10–14) the *X* group increases again, while magnesium decreases, its place being taken by ferrous iron. This process continues with iron replacing magnesium and with a gradual increase in the *X* group until the latest stages in the normal pyroxenes.

The changes in the trend of the pyroxenes can be understood when the structure is considered, and this matter has been discussed by Edwards (1942, p. 598) and by Walker and Poldervaart (1949, p. 643), who have pointed out that the entry of the small Fe<sup>''</sup> ion in place of the larger Ca<sup>''</sup> ion (seen in the middle gabbro pyroxenes) would cause a considerable distortion of the lattice, and that such a replacement would have a limiting value beyond which internal stresses would render the structure unstable. This position appears to be almost reached in pyroxene no. 9, and further enrichment in iron should now take place only at the expense of magnesia. The ferrous ion is slightly larger than the magnesium ion, and thus, as more iron is introduced, the interatomic distances between the chains would be slightly increased. This would further restrict the limits of the iron replacement of calcium, and thus an increasing proportion of calcium ions would again tend to enter the pyroxene structure as the ferrohedenbergite end of the series is approached.

In plutonic rocks, with slow cooling, it may be that the clinopyroxene structure only remains stable when the replacement of calcium by ferrous iron is less than about one-third, and any further replacement by iron must therefore come at the expense of magnesium. The only clinopyroxenes known in which the replacement of calcium by ferrous iron is greater than about a third are the pigeonites and the slag pyroxene described by Bowen (1935). Many of these are the products of rapid crystallization and are probably metastable forms.

#### IV. THE CHANGE IN COMPOSITION OF THE PYROXENES AND THEIR RELATIONS TO THE MAGMA AND THE OTHER MINERAL PHASES.

The clinopyroxenes of the layered series form an unbroken series, and trend lines have been drawn from them based on 19 analyses (fig. 1). Wager and Deer (1939), from the known thermal data of the systems clinoenstatite–diopside, hedenbergite–clinoferrrosilite, and clinoenstatite–clinoferrrosilite, have considered the probable form of the isothermal

surface within the four-component system, and this idea has been further amplified by Hess (1941) who drew a series of hypothetical sections across the area between the Di-Hd and En-Fs joins to show the relations of the lime-rich clinopyroxenes to the pigeonites. These relations

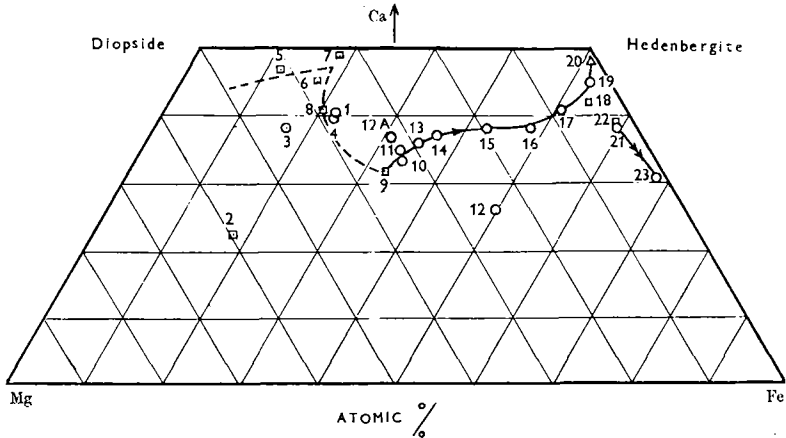


FIG. 1. Trend of clinopyroxenes of the Skaergaard intrusion, east Greenland.

- Chemical analysis of clinopyroxene.
- ◻ Clinopyroxene composition recalculated from analysis of bulk pyroxene of the rock.
- △ Composition estimated from optical determinations.
- Trend of normal pyroxenes, →→ trend of inverted pyroxenes.

indicate a cotectic curve beginning close to the clinoenstatite-diopside join near Wo 45, En 55, and extending towards the hedenbergite-clinoferrrosilite join at Wo 30, Fs 70. As the cotectic curve approaches the two-pyroxene boundary, the solidus and liquidus of the ferroaugites bend slightly downwards and develop into a solid solution series with a minimum, the eutectic between ferroaugite and ferropigeonite becoming a reaction point. From this stage onwards, the field of olivine narrows down the pigeonite field until the latter disappears altogether. From these considerations it is clear that for any position on the liquidus the corresponding solidus point should be nearer to the clinoenstatite-diopside join, and hence the pyroxenes should always show enrichment in magnesia compared with the liquid from which they have crystallized. This is always the case with the Skaergaard pyroxenes.

Because of the strong fractionation of the Skaergaard intrusion, the compositions of the successive liquids and of the pyroxenes with which they are in equilibrium should give the positions of the liquidus and

solidus of the system from near the diopside-clinoenstatite join in the early rocks, to the hedenbergite-clinoferrosilite join in the latest stages. The resemblance between the solidus as determined from the Skaergaard pyroxenes and that deduced from data of artificial systems (Hess, 1941) should be only approximate however, because of the extremely gentle slope of the solidus surface on the lime-rich side of the cotectic curve. Because of this gentle slope of the solidus surface towards the Ca component of the system it is very probable that the position of this cotectic curve and the lime content of the lime-rich solidus phase would be very susceptible to change by:

- (a) the addition of  $Al'''$ ,  $Fe'''$ ,  $Ti'''$ , or similar ions to the solidus phase in any considerable amount;
- (b) structural strains in the pyroxene caused by the replacements of  $Mg''$  and  $Ca''$  by  $Fe''$  (discussed in the previous section);
- (c) the relative amounts of the total Ca, Mg, and Fe from the magma available for incorporation in the pyroxenes (see later).

In a simple 3-component system it is this last factor which determines the position of the cotectic curve; but in a magma, phases such as plagioclase, apatite, olivine, and iron ores are competing for the available Ca, Mg, and Fe from the liquid. All these do not appear in the artificial metasilicate system  $CaSiO_3$ - $MgSiO_3$ - $FeSiO_3$  for which the position of the cotectic curve and slope of the isothermal surface have been deduced.

As  $Al'''$ ,  $Fe'''$ ,  $Ti'''$ , or other ions do not enter the Skaergaard pyroxenes appreciably their effect is likely to be small and so the final position of the cotectic curve should depend mainly on the other two factors. The first of these having been discussed already, attention will now be focused on the other. The crystallization of the clinopyroxenes can be resolved into the variation of three principal components—lime, magnesia, and ferrous iron. As all three are available in the magma in varying amounts throughout the crystallization history, one of the controlling conditions will be the nature of the phases separating at any one time, for the oxides with which the magma is saturated must be shared amongst these.

The lime taken out of the magma enters plagioclase feldspar, monoclinic pyroxene, and apatite. The MgO and FeO are required to form olivine, ortho- and clinopyroxenes, and the iron ores. If the composition of the liquid varies in such a way that it moves out of the field where all these minerals can crystallize in equilibrium with each other, then one phase at least will cease to crystallize. The magma, however, would continue to remain saturated with the components which went to make

up that phase, and with falling temperature these components should be taken up by the remaining minerals which are still being precipitated. Thus, the proportions of the various oxides now entering into these minerals would be altered, and changes in their relative amounts and in composition could be expected in the other minerals which continue to separate when one mineral ceases to crystallize or a new one begins to form.

Wager and Deer (1939, p. 127) considered that the material forming the rocks of the layered series consisted of two parts: (a) the primary precipitate, made up of crystals which separated from the overlying magma; and (b) the interprecipitate material, which crystallized from the magma trapped between the crystals of the primary precipitate. Only one new mineral phase involving lime appears; this is apatite which does not occur in the primary precipitate until a late stage when the  $P_2O_5$  content of the magma has increased to saturation point. The plagioclase feldspar requires less lime as the differentiation proceeds, for it changes in composition from An 60 in the early rocks to An 30 in the latest. The lime content of the liquid decreases from about 11 % in the original magma to 6 % when the latest rocks of the layered series were formed. Hence, there is never any great impoverishment in this constituent in the later stages of the Skaergaard magma.

The ferromagnesian minerals present a somewhat more complicated story. Olivine begins to crystallize in the early rocks of the layered series, but ceases to form during the middle gabbro stage. Its reappearance marks the beginning of the ferrogabbros and it remains as an essential constituent of the rocks until the latest stages when its composition is Fa 98. Orthopyroxene crystallizes in the earliest rocks along with the clinopyroxene and continues to form until some time after the beginning of the lower ferrogabbros. It occurs in the lowest rocks of the layered series, only as an interprecipitate mineral, and here the textures do not suggest that it has inverted from a pigeonite. In the middle gabbros, however, it is intimately associated with the augite and here it is clear that both pyroxenes must have crystallized at the same stage. The orthopyroxene of such rocks contains numerous bleb-like inclusions of lime-rich clinopyroxene and would appear to have inverted from a pigeonite. When the percentage of  $FeSiO_3$  in the orthopyroxenes is plotted against height, and the curve is extrapolated to the height where the mineral disappears, the latest orthopyroxene to form has a composition near Of 70.

Iron ore is present in the early layered rocks only as an interprecipitate

mineral, but it makes its appearance as a mineral of primary precipitation about the end of the hypersthene-olivine-gabbros. Magnetite and ilmenite, the two ores involved, appear to be governed by the amount of  $\text{Fe}_2\text{O}_3$  and  $\text{TiO}_2$ , respectively, available from the magma. Since both these oxides are subtracted from the magma in only small amount in the early rocks, they become concentrated in the later liquids, as does  $\text{P}_2\text{O}_5$ . These two phases appear suddenly in the primary precipitate and take up a certain amount of the available  $\text{FeO}$ .

The chilled margin pyroxene no. 1 is only slightly poorer in lime than the three analysed pyroxenes from the hypersthene-olivine-gabbros and has a higher iron-magnesia ratio. All the analyses of augites from the hypersthene-olivine-gabbros fall into the well-known field of clinopyroxenes from olivine-gabbros and related rocks, and analyses of similar pyroxenes are abundant in the literature. The lowest part of the main-layered series is not exposed, but the pyroxenes from this part of the intrusion must certainly be more magnesian and less iron-rich than pyroxene no. 5. If the earliest rocks of the border group can be considered as analogous with the hidden layered rocks, then these too should contain very magnesian pyroxenes. Such minerals are found in the gabbro-picrite (augite  $\gamma'$  1.698,  $2V$   $58^\circ$ , therefore the composition is approx. Ca 47, Mg 48, Fe 5 atomic %; hypersthene  $2V_\alpha$   $82^\circ$ , and therefore the composition is Of 20) and in the 'perpendicular felspar rock' (augite  $\gamma$  1.702). It would appear, therefore, to be a reasonable assumption that the composition of the pyroxenes of the hidden layered series would lie on the extrapolation of the trend line drawn through analyses 7, 6, and 5 towards the diopside-clinoenstatite join. Such compositions would conform with those of pyroxenes from the Stillwater complex of Montana (Hess, 1949) and of pyroxenes from other very magnesian rocks.

Bowen (1914) who investigated the system clinoenstatite-diopside showed that in the artificial system there was complete solid solution between the end-members. In most igneous rocks, however, two pyroxene phases are normally present and Hess (1941) has suggested that the two-pyroxene field might extend at least to a line close to the diopside-clinoenstatite join before changing over to a series of solid solutions with a minimum. In this connexion the composition of pyroxene no. 2 is of interest. It is a recalculated analysis, and Wager and Deer (1939) suggested that the analysed material might have contained more orthopyroxene than was allowed for and doubted whether the estimated composition of the clinopyroxene was reliable. However, even if there was three times as much orthopyroxene in the analysed

sample as was estimated, its composition would be approximately Ca 30, Mg 60, Fe 10; i.e. the clinopyroxene remains deficient in lime and lies outside the field normal to pyroxenes from such olivine-gabbros. This analysis, therefore, may be regarded as evidence that for very magnesia-rich and iron-poor pyroxenes complete solid solution between pigeonite and diopsidic augites exists. An alternative explanation of the complete miscibility observed between clinoenstatite and diopside in the artificial system and the conflicting evidence in basic magmas was put forward by Tsuboi (1932), who suggested that at lower temperatures diopside and pigeonite would show only limited miscibility, at higher temperatures more miscibility would be shown and that at dry-melt temperatures complete solid solution would be possible. Bowen, Schairer, and Posnjak (1933) discussed this matter further.

At a height of 900 metres in the layered series, i.e. about 20 metres above the level of analysis no. 7, olivine ceases to crystallize as a primary constituent. During the middle gabbro stage, as analyses nos. 8 and 9 show, the pyroxenes become progressively more lime-poor, and while their magnesia contents remain more or less constant or even increase slightly, there is an increase in ferrous iron at the expense of lime. At this stage the composition of the magma has moved from the field where olivine can crystallize together with clinopyroxene into the clinopyroxene field itself, but nevertheless it remains saturated with magnesia, ferrous iron, and silica. The only phases continuing to crystallize which could incorporate all three components are pyroxenes. To some extent the appearance of magnetite and ilmenite in the middle gabbros must reduce the amount of ferrous iron available for the pyroxenes and the presence of the iron ores may in part explain the slight reduction in the iron content of the clinopyroxenes at this stage as shown by analysis no. 8.

If more clinopyroxene of similar lime content were to crystallize in the middle gabbros to incorporate the iron and magnesia now available, the lime content of the magma would be greatly reduced or else the plagioclase to crystallize would have to become more sodic to allow for the additional withdrawal of lime to form pyroxene. If, to compensate for this withdrawal of additional lime to form pyroxene, the amount of plagioclase to crystallize were to be reduced, this in turn would effect the soda, alumina, and silica components of the magma. It is possible, therefore, that the available magnesia and ferrous iron would be taken up by an increase in the amount of clinopyroxene to crystallize, an increase which would at the same time require only the same total

amount of lime from the magma. Therefore the clinopyroxene should become poorer in lime.

Another possible way in which the available iron and magnesia could be taken up would be by an increase in the amount of orthopyroxene to crystallize (as pigeonite). However, during the middle gabbro period the amount of this mineral to crystallize decreases gradually, although it now seems to form in the primary precipitate along with augite and not merely as an interprecipitate mineral as in the lower rocks. Furthermore, when olivine reappears in the ferrogabbros, hypersthene does not disappear at once, but is still found in rocks 150 metres above the level of the reappearance of olivine. These observations do not suggest that there is an intimate relationship between the iron-rich orthopyroxene (or pigeonite) and olivine, a conclusion which is supported by the results obtained by Bowen and Schairer (1935) for the artificial system  $MgO-FeO-SiO_2$ , where the reaction relation between olivine and clinopyroxene disappears for clinopyroxenes containing more than about 25 mol. %  $FeSiO_3$ . In the first analysed ferroaugite after olivine reappears (no. 10) a great change in the direction of the trend is noted however.

Pyroxene no. 10 comes from a rock at a height of 1700 metres in the layered series and olivine makes its appearance some 200 metres lower down. While magnesia once again begins to fall slowly, with increasing height, iron continues to increase, but the most significant change is in the lime content. It can be explained by the incoming of olivine again in significant amount and this would require a large amount of the iron and magnesia available from the magma.

A new analysis has been made of the pyroxene from the type rock of the lower ferrogabbros (1907, Wager and Deer, 1939), for this pyroxene (no. 12) lies away from the new trend line. The new analysis (no. 12A) lies near the trend; the material for this came from the Cambridge specimen. It will be noted that the optical properties of this mineral differ from those quoted for no. 12 (table 2). In order to establish whether the optics of the pyroxene of other collections of this rock agreed with those of the Cambridge specimen,  $\gamma'$  (on cleavage flakes) was determined for the pyroxene from three specimens of the rock from this locality kindly submitted by Professor Wager. It was also determined for the pyroxene from a neighbouring rock (1493). The refractive index  $\gamma'$  for all these specimens agrees within  $\pm 0.003$  with that determined for the analysed specimen no. 12A. It was also decided to check the composition of the olivine in the Cambridge specimen by measurement of the  $\alpha$

refractive index; this gave a value of 1.829, corresponding with 74 molecular per cent. fayalite, whereas Wager and Deer give the composition based both on chemical analysis and on optical data, as Fa 59. This difficulty has not been resolved.

The next change of direction in the trend of the pyroxenes is seen beyond the level of pyroxene no. 13, where the increase in lime content gradually ceases, and the progressive enrichment in iron, with a complementary decrease in magnesia, is even more marked. This causes a gradual flattening of the curve, and this point marks the entry of apatite as a primary phase. The incoming of this mineral seems to depend on the  $P_2O_5$  content of the magma. As no apatite crystallizes in the early stages in the primary precipitate, the  $P_2O_5$  content of the liquid increases until the magma is saturated at about 1.5 %. This new phase, which comes in very suddenly, amounts to 7 % in the parent rock of pyroxene no. 14 and so requires considerable amount of lime. As the total lime available in the liquid continues to decrease, less is available for the pyroxene.

It will be noted that with the incoming of olivine the pyroxene begins to decrease in amount, a decrease which is partly offset by the increase in the lime content of the pyroxene. During this stage, however, the feldspar increases slightly in amount but decreases in its lime content. In this way the lime available from the magma is distributed. At 1850 metres, where apatite makes its appearance, the plagioclase decreases and this too makes lime available for apatite. The pyroxene now begins to increase again, as does olivine, and this is due to the great increase in the iron content of the liquid and to the rapidly decreasing solubility of magnesia in it. This trend in the pyroxenes continues through analyses nos. 15, 16, 17, and 18. The lime content remains about Ca 39 with a slight rising tendency, while Mg decreases from 19 to 8 and at the same time Fe increases from 43 to 55. Apatite and plagioclase feldspar continue to crystallize until after the end of the layered series, although both are decreasing in amount and therefore more and more of the available lime is free for incorporation in the pyroxene.

The brown pyroxene no. 18 shows that for the normal pyroxenes the trend continues with a gradually rising lime content towards the hedenbergite-clinoferrrosillite join, and that in the latest stages where the iron content of the magma is decreasing it turns towards hedenbergite. This is shown by the analysis of the pyroxene no. 19 (from a height of 2800 metres) in the unlamated layered series. The latest stages of the Skaergaard intrusion are represented by hedenbergite-granophyres with

green pyroxenes whose composition must lie very close to hedenbergite itself. The optical properties determined for the pyroxene no. 20 from one of these rocks were  $\alpha$  1.728,  $\beta$  1.735,  $\gamma$  1.756,  $2V$   $56^\circ$ . This mineral is associated with an olivine near fayalite.

In the rocks at a height of about 2350 metres in the layered series the clinopyroxenes develop a very unusual habit for igneous pyroxenes, occurring as patches of interlocking disoriented grains of a green colour instead of the usual brown. These pyroxenes are generally crowded with tiny granular opaque inclusions, and Wager and Deer suggested that they were really inverted forms, having crystallized from the magma as iron-wollastonites. Associated with some of these green pyroxenes, and forming a discontinuous border to them or small internal patches in them, is a brown variety (no. 18) in crystallographic continuity with the green. This pyroxene appears to have formed when the magma temperature was lower than the minimum for the iron-wollastonite-hedenbergite inversion and to have crystallized directly from the magma as a normal pyroxene. The inversion must, therefore, have occurred before crystallization was complete.

The pyroxenes which were thought to have inverted from iron-wollastonites show a very marked reduction in the lime content and contain very small amounts of magnesia. The green pyroxenes from nos. 21 and 22 are very similar and contain only about 0.6 % MgO, whereas the brown pyroxene at this stage (no. 18) carries 1.35 %. Further, although the total iron content in the magma is now beginning to decline, the iron content of these pyroxenes continues to increase, rising from Fe 59 in no. 21 to Fe 68 in no. 23.

Thus, the iron-wollastonites over the range in which they crystallize become progressively more iron rich and lime poor. This is in harmony with the results obtained by Bowen, Schairer, and Posnjak (1933) in the artificial system  $\text{CaO-FeO-SiO}_2$ . Although for iron-rich wollastonites the composition of the mineral cannot be deduced from the simple binary system, the composition of analysis no. 23 corresponds very closely with the point where, with lowest temperature in the system, olivine and iron-rich wollastonite are in equilibrium. This very low content of magnesia in the green pyroxenes at the top of the layered series accounts for the very low magnesia content in the parent rocks at this stage. Analyses of later rocks in the intrusion after the whole of the layered series had ceased to crystallize show that such rocks are somewhat richer in magnesia than the rocks at the top of the layered series. It is now clear that this is due to the higher MgO content of the normal ferroaugites

compared with the iron-wollastonites. A rather unusual feature of the analyses of the inverted pyroxenes is their notable alumina content. Analyses of minerals of the wollastonite group are characterized by very low alumina values, but in the case of these inverted pyroxenes the wollastonites contained notable amounts of ferric iron and the presence of aluminium in the z group is necessary to render the structure electrostatically neutral.

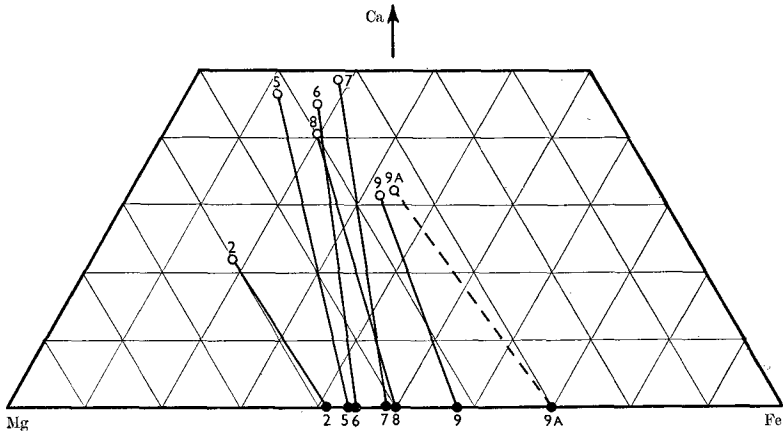


FIG. 2. Relations between clinopyroxenes and their associated orthopyroxenes. Dashed line indicates the limit of the two-pyroxene field. Atomic %.

It is of interest to compare the degree of progressive enrichment of the clinopyroxene in total iron with respect to magnesia, with that of the parent rock and with the similar enrichment in the associated orthopyroxene and olivine. For this the ratio  $(\text{FeO} + \text{Fe}_2\text{O}_3 + 100)/(\text{FeO} + \text{Fe}_2\text{O}_3 + \text{MgO})$  is used (table II). The comparison with the parent rock shows that in all cases the ratio is lower in the pyroxene than it is for the rock, but that with gradual enrichment in iron the difference becomes less and less marked, and in the final stages the ratios are the same.

The relations of the clino- and orthopyroxenes from the same rock are shown in fig. 2. For this diagram the lime content of orthopyroxenes nos. 8 and 9 which are considered to have formed by inversion from pigeonite is not taken into account. From this it can be seen that the orthopyroxene is always richer in ferrous iron with respect to magnesia than the associated clinopyroxene. Even if the Ca component is ignored and the amounts of Mg and Fe are worked out as ratios, then the same enrichment of the orthopyroxene in ferrous iron with respect to

magnesia is seen to hold. This is in keeping with the relations of the two minerals, for the clinopyroxene occurs as a mineral of primary crystallization, whereas the orthopyroxene usually occurs interstitially and crystallized later. As the orthopyroxene had a composition of Of 70 when it finally ceased to crystallize, by interpolation along the trend line, the composition of the monoclinic pyroxene no. 9A at this stage

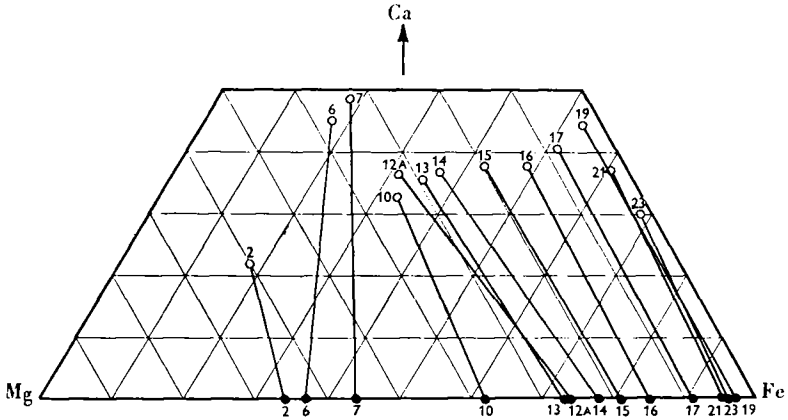


FIG. 3. Relations between clinopyroxenes and their associated olivines. Atomic %.

can be deduced. This is indicated in fig. 2 where the dashed line indicates the limit of the two-pyroxene field. The relations of the two pyroxenes, if the Ca component is ignored and the clinopyroxene is recalculated in terms of Mg and Fe, are shown in table IV.

TABLE IV. Comparison of iron enrichment in associated clinopyroxenes and orthopyroxenes. Atomic %.

Clinopyroxene (Mg and Fe recal. to 100 %)	Fe	23	27	31	35	33	48	50	51
Orthopyroxene	Fe	41	44	45	49	50	58	70	none
No. ...		2	5	6	7	8	9	9A	10

In the case of the olivines, the relation between the clinopyroxenes and their associated olivines is set out diagrammatically in fig. 3. The olivines lag behind the orthopyroxenes in the replacement of Mg by Fe, a relation that is in harmony with the experimental results of Bowen and Schairer (1935). The clinopyroxenes, however, lag behind the olivines in iron enrichment in the early stages, and, with the exception of the reaction-rim olivine associated with pyroxene no. 9 which is more

magnesian than the pyroxene, the olivine remains the more iron rich until we come to the parent rocks of pyroxenes nos. 21 and 23. Here, the explanation for the reversal of the normal relationship is that iron-wollastonite was the actual phase crystallizing from the magma along with the olivine, and this, as we have seen before, was extremely poor in magnesia. The relations between the clinopyroxenes and their associated olivines are shown in table V.

TABLE V. Comparison of iron enrichment in associated clinopyroxenes and olivines. Atomic %.

Clinopyroxene ...	Fe	23	31	35	51	50	55	59	68	80	86	95	96	97
Olivine ...	Fe	34	37	44	62	74	73	78	81	85	91	97	96	96
No. ...		2	6	7	10	12a	13	14	15	16	17	19	21	23

Thus, as we have seen in the Skaergaard intrusion, the orthopyroxene is the most iron-rich ferromagnesian silicate, then comes the olivine, and lastly the clinopyroxene. In general, in other intrusions where the relations between the ferromagnesian minerals have been worked out iron enrichment in the lime-rich clinopyroxene lags behind that of its associated orthopyroxene or pigeonite.

## V. CONCLUSIONS.

It has been shown that data from the artificial systems has enabled a picture to be drawn of solidus liquidus relations in the pyroxenes. The incursion of the olivine field limits the composition of the pigeonite-pyroxene series towards the iron-rich end. The extremely gentle slope of the solidus surface on the lime-rich side of the cotectic curve renders the lime content of the clinopyroxene extremely sensitive to alteration by the following factors:

- (a) the amount of Al, Fe<sup>'''</sup>, and Ti taken into solid solution;
- (b) internal strains in the mineral structure caused by replacement of Ca and Mg by Fe<sup>''</sup>;
- (c) by the proportions of Ca, Mg, and Fe<sup>''</sup> available from the magma to form the clinopyroxene. In the case of the Skaergaard clinopyroxenes this last factor is considered to be the most important.

The two abrupt changes in the direction of the trend in the clinopyroxene are attributed to the disappearance of olivine as a primary phase and its later sudden reappearance in the lower ferrogabbro stage. The flattening out of the trend line in the middle of the ferrogabbros may be correlated with crystallization of apatite in large amount as a primary mineral.

In the latest stages two distinct trends can be made out. That of the normal ferroaugites finally turns towards hedenbergite as the iron content of the magma begins to decline and the pyroxenes are green in colour at this stage. The other trend is that of the pyroxenes derived from the iron-wollastonite-hedenbergite inversion. Here the pyroxenes become progressively more iron rich and lime poor and magnesia is reduced to insignificant amounts. The final pyroxene has a composition Ca 30, Fe 70, which corresponds to the position deduced for the lowest-temperature relations in the hedenbergite-clinofersosilite series of the artificial system.

A discussion of the significance of the Skaergaard clinopyroxene trend and comparisons with the pyroxenes from other tholeiitic rocks will be made in a later communication.

*Acknowledgements.*—The author desires to thank Professors L. R. Wager and W. A. Deer for permission to work on their material, and Professor C. E. Tilley, Professor W. A. Deer, Dr. S. R. Nockolds, and Dr. N. F. M. Henry for their interest, advice, and helpful criticism in connexion with this paper.

#### APPENDIX.

*Note on the relationship of the optical properties to the chemical composition in clinopyroxenes.*

Many attempts have been made to correlate the optical properties of clinopyroxenes with their chemical compositions and Tomita (1934) first drew up a set of diagrams showing variations in refractive indices, optic axial angle, and extinction angles. Later these were modified by Deer and Wager (1938). Hess (1949), in a paper which lists many new chemical analyses together with very accurate optical determinations, has drawn up new tables showing the variation in refractive indices, optical axial angle, and the birefringence for common clinopyroxenes. He considered that his diagrams were most reliable for those areas where natural pyroxenes are commonest and that natural pyroxenes were rare or did not exist where his data are poor. The exception was the ferroaugite field where Hess's curves were based on only seven analyses, two of which contain significant amounts of soda and so should be rejected for 2V curves. For the present paper many new analyses of ferroaugites have been carried out and new refractive index and 2V curves have been drawn. These should improve on the accuracy of Hess's curves for the ferroaugite field, but elsewhere they agree very closely with his diagram. The writer has followed Hess in using atomic % Ca, Mg, Fe

to express the compositions of pyroxenes and has found the recognition and use of the (100) parting tablets, advocated in the 1949 paper, the most convenient and rapid method of determining a refractive index of a clinopyroxene. The new curves are presented in fig. 4.

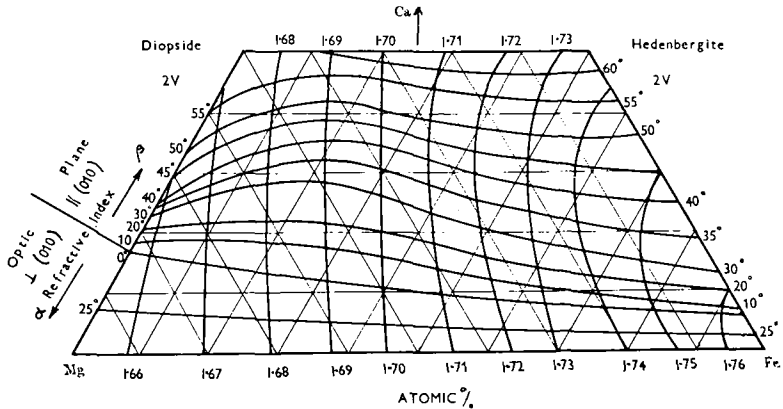


FIG. 4. Relation between the chemical composition of clinopyroxenes and the values of  $2V$  and the refractive index along the  $b$  crystallographic axis.

#### References.

- BARTH (T. F. W.), 1931. Pyroxen von Hiva Oa, Marquesas-Inseln und die Formel titanhaltiger Augit. *Neues Jahrb. Min., Abt. A*, vol. 64, pp. 217-224. [M.A. 5-219.]
- BOWEN (N. L.), 1914. The system diopside-forsterite-silica. *Amer. Journ. Sci.*, ser. 4, vol. 38, pp. 207-264.
- 1935. "Ferrosilite" as a natural mineral. *Amer. Journ. Sci.*, ser. 5, vol. 30, pp. 481-494. [M.A. 6 260.]
- and SCHAIRER (J. F.), 1935. The system  $MgO \cdot FeO \cdot SiO_2$ . *Amer. Journ. Sci.*, ser. 5, vol. 29, pp. 151-247. [M.A. 6-352.]
- SCHAIRER (J. F.), and POSNJAK (E.), 1933. The system  $CaO \cdot FeO \cdot SiO_2$ . *Amer. Journ. Sci.*, ser. 5, vol. 26, pp. 193-284. [M.A. 5-454.]
- DEER (W. A.) and WAGER (L. R.), 1938. Two new pyroxenes included in the system clinoenstatite, clinoferrosilite, diopside, and hedenbergite. *Min. Mag.*, vol. 25, pp. 15-22.
- DIXON (B. E.) and KENNEDY (W. Q.), 1933. Optically un axial titanaugite from Aberdeenshire. *Zeits. Krist.*, vol. 36, pp. 112-120. [M.A. 5-440.]
- EDWARDS (A. B.), 1942. Differentiation in the dolerites of Tasmania. *Journ. Geol.*, vol. 50, pp. 451-480, 579-610. [M.A. 9-161.]
- HENRY (N. F. M.), 1935. Some data on the iron-rich hypersthene. *Min. Mag.*, vol. 24, pp. 221-226.
- HESS (H. H.), 1941. Pyroxenes of common mafic magmas. *Amer. Min.*, vol. 26, pp. 515-555, 573-579. [M.A. 8-233.]
- 1949. Chemical composition and optical properties of common clinopyroxenes. *Amer. Min.*, vol. 34, pp. 621-666. [M.A. 11-15.]

- KENNEDY (G. C.), 1949. Equilibrium between volatiles and iron oxides in igneous rocks. *Amer. Journ. Sci.*, vol. 246, pp. 529-549. [M.A. 10-424.]
- KENNEDY (W. Q.), 1933. Trends of differentiation in basaltic magmas. *Amer. Journ. Sci.*, ser. 5, vol. 25, pp. 239-256.
- POLDERVAART (A.), 1944. The petrology of the Elephants' Head dyke and the New Amalfi sheet. *Trans. Roy. Soc. South Africa*, vol. 30, pp. 85-119.
- TILLEY (C. E.), 1950. Some aspects of magmatic evolution. *Quart. Journ. Geol. Soc. London*, vol. 106, pp. 37-61.
- TOMITA (T.), 1934. Variations in optical properties, according to chemical composition, in the pyroxenes . . . *Journ. Shanghai Sci. Inst.*, sect. 2, vol. 1, pp. 41-58. [M.A. 6-71.]
- TSUBOI (S.), 1932. On the course of crystallization of pyroxenes from rock-magmas. *Japanese Journ. Geol. Geogr.*, vol. 10, pp. 67-82. [M.A. 5-219.]
- WAGER (L. R.) and DEER (W. A.), 1939. Geological investigations in east Greenland, Part III. Petrology of the Skaergaard intrusion, Kangerdlugssuaq, east Greenland. *Medd om Grønland*, vol. 105, no. 4, pp. 1-352. [M.A. 8-27.]
- WALKER (F.) and POLDERVAART (A.), 1949. The Karroo dolerites of the Union of South Africa. *Bull. Geol. Soc. Amer.*, vol. 60, pp. 591-705. [M.A. 11-32.]
- WARREN (B. E.) and BISCOE (J.), 1931. The crystal structure of the monoclinic pyroxenes. *Zeits. Krist.*, vol. 80, pp. 391-401. [M.A. 5-186.]
- and BRAGG (W. L.), 1928. The structure of diopside,  $\text{CaMg}(\text{SiO}_3)_2$ . *Zeits. Krist.*, vol. 69, pp. 168-193. [M.A. 4-31.]
-